



**UNIVERSITI PUTRA MALAYSIA**

***ELECTROCHEMICAL PROPERTIES OF MODIFIED TITANIA  
NANOTUBES INCORPORATED WITH  $Mn_2O_3$  AND  $Co_3O_4$  FOR  
SUPERCAPACITOR APPLICATION***

**NURUL ASMA BINTI SAMSUDIN**

**FS 2017 68**



**ELECTROCHEMICAL PROPERTIES OF MODIFIED TITANIA  
NANOTUBES INCORPORATED WITH  $\text{Mn}_2\text{O}_3$  AND  $\text{Co}_3\text{O}_4$  FOR  
SUPERCAPACITOR APPLICATION**

By

**NURUL ASMA BINTI SAMSUDIN**

**Thesis Submitted to the School of Graduate Studies,  
Universiti Putra Malaysia, in Fulfilment of the Requirements for the Degree of  
Doctor of Philosophy**

**June 2017**

All material contained within the thesis, including without limitation text logos, icons, photographs and all other artwork, is copyright material of Universiti Putra Malaysia unless otherwise stated. Use may be made of any material contained within the thesis for non-commercial purposes from the copyright holder. Commercial use of material may only be made with the express, prior, written permission of Universiti Putra Malaysia.

Copyright© Universiti Putra Malaysia



Dedicated with much respect and gratefulness to  
the love of my life after Allah and Prophet Muhammad, my beloved parents.



Abstract of this thesis presented to the Senate of Universiti Putra Malaysia in fulfilment of the requirement for the degree of Doctor of Philosophy

**ELECTROCHEMICAL PROPERTIES OF MODIFIED TITANIA  
NANOTUBES INCORPORATED WITH  $\text{Mn}_2\text{O}_3$  AND  $\text{Co}_3\text{O}_4$  FOR  
SUPERCAPACITOR APPLICATION**

By

**NURUL ASMA BINTI SAMSUDIN**

**June 2017**

**Chairman: Professor Zulkarnain Zainal, PhD**  
**Faculty : Science**

Highly ordered titania nanotubes (TNTs) was used in this study as it known to have a remarkable chemical stability and its open ended nanotubes structure offers large surface area and good interfacial connectivity with the electrolyte which will enhance the capacitive performance. The TNTs were synthesised by electrochemical anodisation method in two-electrode cell containing  $\text{NH}_4\text{F}$  solution. Parameters affecting the morphological and geometrical aspects as well as electrochemical performance of TNTs were investigated by varying the electrolyte composition, applied anodisation voltage and anodisation time. The formation of TNTs were confirmed by x-ray diffraction (XRD) and field emission scanning electron microscopy (FESEM) analyses. Meanwhile the electrochemical performance of the TNTs were evaluated in 1.0 M KCl electrolyte using cyclic voltammetry (CV) and galvanostatic charge-discharge test in a three electrode electrochemical cell system consisted of Pt as counter electrode, Ag/AgCl (3 M KCl) electrode as reference electrode and TNTs as the working electrode.

Single phase anatase TNTs were obtained upon calcination at 500 °C for samples prepared at all electrolyte compositions. FESEM revealed the nanotubes formed were uniform with well defined circular tubes. However, the tubes becomes disordered and clustered with irregular shape as the water content increased. All prepared TNTs displayed reversible unsymmetrical CV shapes with distorted anodic region and this was associated to the non-faradic charge-discharge of the oxide surface. TNTs 5 % exhibits highest current which leads to higher capacitance compared to other synthesised samples.

TNTs 5% was further modified by electrochemical reduction to enhance the capacitive properties. The applied voltage and reduction time were varied to obtain the optimum

condition. Excellent electrochemical performance of modified TNTs 5 % denoted as R-TNTs was observed with CV curve indicated 18 times higher in specific capacitance value than unmodified TNTs. Ideal capacitor behaviour and good electrochemical stability were observed for sample synthesised at applied voltage of 5 V for 30 s. A high average specific capacitance of  $11.12 \text{ mF cm}^{-2}$  was also observed from galvanostatic charge-discharge analysis. The enhancement of the capacitive performance can be attributed to the enhancement in conductivity and electrical performance of the sample due to the introduction of oxygen vacancy by conversion of  $\text{Ti}^{4+}$  to  $\text{Ti}^{3+}$  as revealed by X-ray photoelectron spectroscopy (XPS).

Pulse reverse electrodeposition was applied to deposit  $\text{Mn}_2\text{O}_3$  and  $\text{Co}_3\text{O}_4$  nanoparticles into the R-TNTs to further improve the capacitive performance of the samples. Electrodeposition parameter such as deposition potential, duty cycle, deposition time, concentration of metal precursor, pH of the metal precursor solution and heating temperature were varied to obtain the optimum samples XRD analysis confirmed that  $\text{Mn}_2\text{O}_3$  and  $\text{Co}_3\text{O}_4$  nanoparticles were successfully loaded into the R-TNTs while FESEM and TEM images revealed the presence of the nanoparticles along the R-TNTs tubes wall. Specific capacitance, as high as  $37.00 \text{ mF cm}^{-2}$  obtained for  $\text{Mn}_2\text{O}_3/\text{R-TNTs}$  and  $16.89 \text{ mF cm}^{-2}$  for  $\text{Co}_3\text{O}_4/\text{R-TNTs}$  due to the contribution of double-layered capacitance by the R-TNTs and pseudocapacitance of the metal oxides. The synthesised samples displayed a good electrochemical stability as they exhibits more than 85% capacitive retention after 1000 charge-discharge cycles.

Abstrak tesis yang dikemukakan kepada Senat Universiti Putra Malaysia  
sebagai memenuhi keperluan untuk ijazah Doktor Falsafah

**SIFAT ELEKTROKIMIA TITANIA NANOTIUB TERUBAH SUAI YANG  
DIMUATKAN DENGAN  $Mn_2O_3$  DAN  $Co_3O_4$  UNTUK APLIKASI  
SUPERKAPASITOR**

Oleh

**NURUL ASMA BINTI SAMSUDIN**

**Jun 2017**

**Pengerusi:      Profesor Zulkarnain Zainal, PhD**  
**Fakulti    :      Sains**

Titania nanotub yang tersusun rapi (TNTs) telah digunakan dalam kajian ini kerana diketahui memiliki ciri yang luar biasa termasuk kestabilan kimia dan struktur nanotubnya yang berhujung terbuka menawarkan permukaan yang luas dan boleh menyediakan kesalinghubungan yang lebih baik antara bahan aktif dan elektrolit yang akan meningkatkan prestasi kapasitans. TNTs telah disediakan melalui elektrokimia penganodan dalam sel dua elektrod yang mengandungi larutan  $NH_4F$ . Parameter yang mempengaruhi morfologi, aspek geometri dan prestasi elektrokimia TNTs telah dikaji dengan mengubah komposisi elektrolit, voltan penganodan yang digunakan dan tempoh masa penganodan. Pembentukan TNTs telah disahkan dengan analisis pembelauan sinar-X (XRD) dan mikroskopi medan pancaran pengimbasan elektron (FESEM). Prestasi elektrokimia bagi TNTs telah dinilai menggunakan voltametri berkitar, galvanostat cas nyahcas dan spektroskopi elektrokimia impedans dalam sistem sel tiga elektrod yang terdiri daripada Pt sebagai elektrod kawalan,  $Ag/AgCl$  (3 M  $KCl$ ) sebagai elektrod rujukan dan TNTs sebagai elektrod kerja. Ketiga-tiga analisis dilakukan dalam larutan  $KCl$  (1.0 M).

Fasa tunggal titania telah diindekskan kepada anatase bagi kesemua sampel yang telah dikalsin pada suhu 500 °C. FESEM analisis juga menunjukkan bahawa TNTs 5 % menghasilkan tiub yang lebih seragam dan bulat. Namun, bentuk tiub menjadi tidak seragam dan berkelompok apabila kandungan air meningkat didalam elektrolit. Semua sampel TNTs menunjukkan bentuk CV yang tidak simetri dimana bahagian anod terherot yang dikaitkan dengan cas nyahcas tidak faraday oleh permukaan oksida. TNTs 5 % menghasilkan arus yang paling tinggi yang menghasilkan kapasitans yang lebih tinggi berbanding sampel lain.

Pengubahsuaian TNTs 5 % bagi meningkatkan prestasi kapasitans sampel tersebut telah dilakukan melalui kaedah penurunan elektrokimia. Voltan dan masa penurunan yang digunakan telah diubah untuk mendapatkan sampel yang optimum. Prestasi elektrokimia yang baik bagi sampel TNTs 5 % yang telah diubah suai (dinamakan sebagai R-TNTs) dapat diperhatikan melalui lengkung CV yang menunjukkan 18 kali ganda lebih tinggi dari segi kapasitans tentu berbanding dengan TNTs yang tidak diubah suai. Ciri kapasitor ideal dan kestabilan elektrokimia yang baik diperlihatkan bagi sampel yang disintesis pada voltan 5 V selama 30 saat. Kapasitans tentu yang tinggi iaitu  $11.12 \text{ mF cm}^{-2}$  juga diperlihatkan melalui galvanostat cas nyahcas analisis bagi sampel ini iaitu kira-kira 57 kali ganda lebih tinggi daripada TNTs yang tidak diubah suai. Peningkatan prestasi kapasitans ini dikaitkan dengan peningkatan kekonduksian dan prestasi elektrik sampel disebabkan oleh adanya kekosongan oksigen hasil daripada penurunan  $\text{Ti}^{4+}$  kepada  $\text{Ti}^{3+}$  seperti yang dibuktikan oleh sinar fotoelektron-X spektroskopi (XPS).

Pengelektroenapan denyut berbalik telah digunakan untuk pengenanapan  $\text{Mn}_2\text{O}_3$  dan  $\text{Co}_3\text{O}_4$  nanopartikel ke atas R-TNTs untuk meningkatkan prestasi kapasitans sampel. Pparameter pengelektroenapan seperti keupayaan enapan, kitaran kerja, masa enapan, kepekatan elektrolit logam, pH elektrolit logam dan suhu pemanasan telah dipelbagaikan untuk mendapat sampel yang optimum. Analisis melalui XRD mengesahkan  $\text{Mn}_2\text{O}_3$  dan  $\text{Co}_3\text{O}_4$  nanopartikel telah berjaya dienap ke atas R-TNTs manakala imej daripada FESEM dan TEM membuktikan kehadiran  $\text{Mn}_2\text{O}_3$  dan  $\text{Co}_3\text{O}_4$  nanopartikel disepanjang dinding tiub R-TNTs. Kapasitans tentu setinggi  $37.00 \text{ mF cm}^{-2}$  diperolehi oleh  $\text{Mn}_2\text{O}_3/\text{R-TNTs}$  dan  $16.89 \text{ mF cm}^{-2}$  oleh  $\text{Co}_3\text{O}_4/\text{R-TNTs}$  disebabkan oleh kapasitans dua lapisan yang dimiliki oleh R-TNTs dan pseudokapasitans dimiliki oleh logam oksida. Kesemua sampel yang disintesis memaparkan kestabilan elektrokimia yang baik kerana mengekalkan lebih daripada 85 % kapasitans selepas melalui cas nyahcas sehingga 1000 kali.



## ACKNOWLEDGEMENTS

First of all, thank you to Allah the almighty for His bless and strength throughout this journey. My deep gratitude and sincere thanks goes to my supervisor Professor Dr. Zulkarnain Zainal for his brilliant insight, invaluable guidance, support, patience, and continuous supervision throughout my study. I wish to express my sincere appreciation to my co-supervisors, Associate Professor Dr. Janet Lim Hong Ngee and Dr. Yusran Sulaiman for their supportive advices, guidance and insightful comments in ensured my continuous enthusiasm for this study. The constructive ideas, guidance and immense knowledge from Dr. Lim Ying Chin are indeed appreciable.

Special thanks are credited to staffs of Microscopy Unit, Institute of Bioscience, Universiti Putra Malaysia, Faculty of Science, Universiti Teknologi Mara and Failure Analysis Laboratory, MIMOS Berhad for their helps in conducting FESEM, EDX, TEM and XPS analysis on my samples. I would like to thank Dr. Chang Sook Keng for her helps, guidance and meaningful discussion about electrochemistry and supercapacitor. Many thanks to Chia Chew Ping and Saudah for their guidance in XRD analysis and data interpretation. My appreciation to my labmates, who supported me from the initial to the final level of this project. Their helpfulness, kindness and friendship have boosted me morally throughout this study. To warda and elmi, thank you very much for the support, foods, memories, vitamin k and j and 2 days 1 night road trips. Many thanks to my PhD financial support from Ministry of Higher Education, Malaysia for this golden opportunity for me to further my study in this prestigious university.

Lastly, special thanks to my brothers, sister and sister in laws for lending their ears and shoulder every time I accounted hardship, their encouragement and love always give me strength to make another step forward. To my nieces and nephews, you are my vitamins, thank you for never fail to make me energised, especially throughout my study. Infinite thanks to my parents Hj. Samsudin Mat Ali and Hjh Wan Zabadah Yusof for their endless love, prayers and support throughout these 4 years journey. Thank you for your understanding for allowing me to peruse my third degree. I never would made it here without your prayers and blessings.

Thank you so much. May Allah gather us in Jannahtul Firdaus.

This thesis was submitted to the Senate of Universiti Putra Malaysia and has been accepted as fulfilment of the requirement for the degree of Doctor of Philosophy. The members of the Supervisory Committee were as follows:

**Zulkarnain Zainal, PhD**

Professor  
Faculty of Science  
Universiti Putra Malaysia  
(Chairman)

**Janet Lim Hong Ngee, PhD**

Associate Professor  
Faculty of Science  
Universiti Putra Malaysia  
(Member)

**Yusran Sulaiman, PhD**

Associate Professor  
Faculty of Science  
Universiti Putra Malaysia  
(Member)

---

**ROBIAH BINTI YUNUS, PhD**

Professor and Dean  
School of Graduate Studies  
Universiti Putra Malaysia

Date:

## TABLE OF CONTENTS

	Page
<b>ABSTRACT</b>	i
<b>ABSTRAK</b>	iii
<b>ACKNOWLEDGEMENTS</b>	v
<b>APPROVAL</b>	vi
<b>DECLARATION</b>	viii
<b>LIST OF TABLES</b>	xiii
<b>LIST OF FIGURES</b>	xv
<b>LIST OF ABBREVIATIONS</b>	xxiii
 <b>CHAPTER</b>	
 <b>1 INTRODUCTION</b>	
1.1 General Introduction	1
1.2 Problem Statement	2
1.3 Background of Study	4
1.4 Objectives of the Study	5
 <b>2 LITERATURE REVIEW</b>	
2.1 Background of Supercapacitor	6
2.2 Current Research Attempts	8
2.3 Charge Storage Mechanisms of Supercapacitor	9
2.3.1 Electric Double Layer Capacitor	10
2.3.2 Pseudocapacitors	11
2.4 Synthesis of Titania Nanotubes (TNTs)	11
2.4.1 Sol-gel Method	12
2.4.2 Hydrothermal Method	12
2.4.3 Atomic Layer Deposition	13
2.4.4 Electrochemical Anodisation Method	13
2.5 Modification of Titania Nanotubes	18
2.5.1 Electrochemical and Thermal Approaches	18
2.5.2 Metal and Conducting Polymers Doping Approach	19
2.6 Electrochemical Deposition	21
2.6.1 Cyclic Voltammetry Electrodeposition	23
2.6.2 Potentiostatic Electrodeposition	25
2.6.3 Pulse Electrodeposition	26
 <b>3 METHODOLOGY</b>	
3.1 Synthesis of Titania Nanotubes (TNTs)	28
3.1.1 Influence of Water Content	29
3.1.2 Influence of Anodisation Voltage and Time	29
3.2 Modification Titania Nanotubes by Electrochemical Reduction Method	29

3.3	Synthesis of R-TNTs/Mn <sub>2</sub> O <sub>3</sub> and R-TNTs/Co <sub>3</sub> O <sub>4</sub> by Pulse Reverse Electrodeposition	30
3.3.1	Cyclic Voltammetry (CV) Analysis of the Electrolyte	31
3.3.2	Variation of Pulse Potential	31
3.3.3	Variation of Duty Cycle	31
3.3.4	Variation of Deposition Time	32
3.3.5	Variation of Electrolyte Concentration	32
3.3.6	Variation of Electrolyte pH	32
3.3.7	Variation of Drying Temperature	32
3.4	Characterizations of TNTs, R-TNTs, Mn <sub>2</sub> O <sub>3</sub> /R-TNTs and Co <sub>3</sub> O <sub>4</sub> /R-TNTs.	33
3.4.1	X-Ray Diffractometry (XRD) Analysis	33
3.4.2	Field Emission Scanning Electron Microscopy (FESEM) and Energy-Dispersive X-Ray Spectroscopy (EDX)	33
3.4.3	Transmission Electron Microscopy (TEM)	33
3.4.4	X-Ray Photoelectron Spectroscopy (XPS)	34
3.5	Electrochemical Measurements	34
3.5.1	Cyclic Voltammetry	34
3.5.2	Galvanostatic Charge-Discharge Test and Ragone Plots	34
3.5.3	Cycle Stability Test	35
3.5.4	Electrochemical Impedance Spectroscopy (EIS)	36
<b>4</b>	<b>RESULTS AND DISCUSSION</b>	
4.1	Synthesis of Titania Nanotubes (TNTs)	37
4.1.1	Influence of Water Content in the Electrolyte	37
4.1.2	Influence of Applied Voltage	47
4.1.3	Influence of Anodisation Time	52
4.2	Modification of Titania Nanotubes by Electrochemical Reduction Method	55
4.2.1	Field Emission Scanning Electron Microscope (FESEM) and Energy-Dispersive X-Ray Spectroscopy (EDX)	55
4.2.2	X-Ray Diffraction (XRD)	57
4.2.3	X-Ray Photoelectron Spectroscopy (XPS)	58
4.2.4	Electrochemical Measurements	59
4.3	Synthesis of R-TNTs/Mn <sub>2</sub> O <sub>3</sub> and Co <sub>3</sub> O <sub>4</sub> /R-TNTs by Pulse Reverse Electrodeposition	64
4.3.1	Determination of Pulse Potential Range for Electrodeposition of Mn <sub>2</sub> O <sub>3</sub> and Co <sub>3</sub> O <sub>4</sub> on R-TNTs	65
4.3.2	Pulse Reverse Electrodeposition of Mn <sub>2</sub> O <sub>3</sub> /R-TNTs and Co <sub>3</sub> O <sub>4</sub> /R-TNTs on R-TNTs	67
4.3.3	Field Emission Scanning Electron Microscope (FESEM) and Energy-Dispersive X-Ray Spectroscopy (EDX)	69
4.3.4	X-Ray Diffraction (XRD)	86

4.3.5	Transmission Electron Microscopy (TEM) of $\text{Mn}_2\text{O}_3/\text{R-TNTs}$ and $\text{Co}_3\text{O}_4/\text{R-TNTs}$	87
4.3.6	Electrochemical Measurements of $\text{Mn}_2\text{O}_3/\text{R-TNTs}$ and $\text{Co}_3\text{O}_4/\text{R-TNTs}$	89
4.4	Comparison Study of TNTs, R-TNTs, $\text{Mn}_2\text{O}_3/\text{R-TNTs}$ and $\text{Co}_3\text{O}_4/\text{R-TNTs}$	120
4.4.1	Ragone Plot	120
4.4.2	Cycle ability Test	121
4.4.3	Electrochemical Impedance Spectroscopy	124
<b>5</b>	<b>CONCLUSION AND RECOMMENDATIONS FOR FUTURE RESEARCH</b>	
5.1	Conclusion	127
5.2	Recommendations for Future Research	128
	<b>REFERENCES</b>	130
	<b>APPENDICES</b>	142
	<b>BIODATA OF STUDENT</b>	154
	<b>LIST OF PUBLICATIONS</b>	155

## LIST OF TABLES

Table	Page
2.1 Comparisons between batteries and supercapacitors.	7
3.1 List of parameters varied in modification of TNTs by electrochemical reduction.	30
3.2 The duty cycle setup for overall on time of 5 min.	31
3.3 The pulse electrodeposition setup for variation of electrolyte pH.	32
4.1 Thickness of TNTs synthesised in various anodisation time.	53
4.2 Summary of optimum condition for synthesis of TNTs	55
4.3 Elemental analysis for Co <sub>3</sub> O <sub>4</sub> /R-TNTs deposited at different potential.	72
4.4 Average inner diameter and wall thickness of Co <sub>3</sub> O <sub>4</sub> /R-TNTs deposited at different potential.	73
4.5 Elemental analysis for Mn <sub>2</sub> O <sub>3</sub> /R-TNTs as function of duty cycle.	74
4.6 Average inner diameter and wall thickness of Co <sub>3</sub> O <sub>4</sub> /R-TNTs deposited at potential -0.90 V using 10 % duty cycle at different deposition time.	82
4.7 Average inner diameter and wall thickness of Co <sub>3</sub> O <sub>4</sub> /R-TNTs deposited at various electrolyte concentration at potential of -0.90 V using 10 % duty cycle for 10 min.	84
4.8 Summary of inner tube diameter and wall thickness of R-TNTs, Mn <sub>2</sub> O <sub>3</sub> /R-TNTs and Co <sub>3</sub> O <sub>4</sub> /R-TNTs.	89
4.9 Specific capacitance of Mn <sub>2</sub> O <sub>3</sub> /R-TNTs and Co <sub>3</sub> O <sub>4</sub> /R-TNTs deposited at different pulse potential obtained from CV and galvanostatic charge-discharge at scan rate of 5 mV s <sup>-1</sup> current density of 0.1 mA cm <sup>-2</sup> .	95
4.10 Specific capacitance of Mn <sub>2</sub> O <sub>3</sub> /R-TNTs and Co <sub>3</sub> O <sub>4</sub> /R-TNTs deposited at different duty cycle obtained from CV and galvanostatic charge-discharge at scan rate of 5 mV s <sup>-1</sup> current density of 0.1 mA cm <sup>-2</sup> .	102

4.11	Specific capacitance of $\text{Mn}_2\text{O}_3/\text{R-TNTs}$ and $\text{Co}_3\text{O}_4/\text{R-TNTs}$ deposited at different deposition time obtained from CV and galvanostatic charge-discharge at scan rate of $5 \text{ mV s}^{-1}$ current density of $0.1 \text{ mA cm}^{-2}$ .	106
4.12	Specific capacitance of $\text{Mn}_2\text{O}_3/\text{R-TNTs}$ and $\text{Co}_3\text{O}_4/\text{R-TNTs}$ deposited at different electrolyte concentration obtained from CV and galvanostatic charge-discharge at scan rate of $5 \text{ mV s}^{-1}$ current density of $0.1 \text{ mA cm}^{-2}$ .	111
4.13	Optimum parameter for pulse electrodeposition of $\text{Mn}_2\text{O}_3/\text{R-TNTs}$ and $\text{Co}_3\text{O}_4/\text{R-TNTs}$	120
4.14	Cell-electrolyte resistance ( $R_s$ ), charge-transfer resistance ( $R_{ct}$ ) and diameter semicircle of TNTs, R-TNTs, $\text{Mn}_2\text{O}_3/\text{R-TNTs}$ / and $\text{Co}_3\text{O}_4/\text{R-TNTs}$ obtained from impedance analysis.	126

## LIST OF FIGURES

Figure		Page
1.1	Overview of the study	5
2.1	Ragone plot of current energy storage and conversion devices	6
2.2	Trends in peer-reviewed publications and resulting citations in major science and engineering journals as stated in ISI Web of Science Database	8
2.3	Schematic of charge storage via (a) EDLC and (b) pseudocapacitance	10
2.4	The fabrication method for TNTs	12
2.5	The electrochemical anodisation setup	14
2.6	(a) Mechanisms of oxide formation on the metal sheet, (b) Metallic titanium morphologies obtained by electrochemical anodisation-compact oxide film, disordered nanoporous layer, a self-ordered nanoporous or self-ordered nanotubes layer, (c) Mechanism o of nanotubes formation	14
2.7	Decorating approach on modification of TNTs.	19
2.8	FESEM images of top view and cross-sections of (a, a') deposited of NiO into TNTs via one-cycle, (b, b') multi-cycle electrodeposition-oxidation synthesis, (c, c') hydrothermal synthesis and (d, d') electrochemical synthesis	20
2.9	Overall reaction in in the electrolyte and electrode/electrolyte interface during the electrodeposition process	22
2.10	Schematic diagram of the electric double-layer	23
2.11	Typical cyclic voltammogram for the reversible redox reaction.	24
2.12	Schematic representation of the potentiostatic electrodeposition.	25
2.13	Schematic representation of the pulse electrodeposition.	26
3.1	Schematic diagram of titanium foil with dimension of 10 mm x 20 mm.	28
3.2	Set up for anodisation experiment.	29



3.3	Schematic illustration of overall synthesis of the samples.	30
3.4	The Nyquist representation of impedance data	36
4.1	FESEM images of TNTs synthesised in $\text{NH}_4\text{F}/\text{EG}$ 5 vol % of $\text{H}_2\text{O}$ using anodisation voltage 20 V for 1 hr; Top view of TNTs (a) before ultrasonication, (b) cross-sectional view.	38
4.2	(a) Top view and (b) cross-sectional view FESEM images of TNTs synthesised in $\text{NH}_4\text{F}/\text{EG}$ 25 vol % of $\text{H}_2\text{O}$ using anodisation voltage 20 V for 1 hr.	39
4.3	(a) Top view and (b) cross-sectional view FESEM images of TNTs synthesised in $\text{NH}_4\text{F}/\text{EG}$ 50 vol % of $\text{H}_2\text{O}$ using anodisation voltage 20 V for 1 hr.	39
4.4	(a) Top view and (b) cross-sectional view FESEM images of TNTs synthesised in $\text{NH}_4\text{F}/\text{EG}$ 75 vol % of $\text{H}_2\text{O}$ using anodisation voltage 20 V for 1 hr.	40
4.5	(a) Top view and (b) cross-sectional view FESEM images of TNTs synthesised in $\text{NH}_4\text{F}/\text{EG}$ 100 vol % of $\text{H}_2\text{O}$ using anodisation voltage 20 V for 1 hr.	40
4.6	Tubes diameter distribution histogram of TNTs synthesised in $\text{NH}_4\text{F}/\text{EG}$ with different water content (b) 100 vol %, (c) 75 vol %, (d) 50 vol %, (e) 25 vol %, (f) 5 vol % of $\text{H}_2\text{O}$ .	41
4.7	Tube diameter versus water content for TNTs anodised at applied voltage 20 V for 1 hr in electrolyte containing different vol. % of $\text{H}_2\text{O}$ .	42
4.8	XRD patterns of (a) as-anodised TNTs and TNTs synthesised in $\text{NH}_4\text{F}/\text{EG}$ with different water content (b) 100 vol %, (c) 75 vol %, (d) 50 vol %, (e) 25 vol %, (f) 5 vol % of $\text{H}_2\text{O}$ . Noted that A and Ti represent anatase and titanium, respectively.	43
4.9	Cyclic voltammograms for TNTs synthesised in $\text{NH}_4\text{F}/\text{EG}$ with different water content 5 to 100 vol. % using anodisation voltage of 20 V for 1 hr at the scan rate of $5 \text{ mV s}^{-1}$ in 1 M KCl.	44
4.10	Cyclic voltammograms for TNTs 5 % using anodisation voltage 20 V for 1 hr at different scan rate in 1 M KCl.	45
4.11	Galvanostatic charge-discharge for TNTs synthesised in $\text{NH}_4\text{F}/\text{EG}$ with different water content 5 to 100 vol. % using anodisation voltage 20 V for 1 hr at current density of $2 \mu\text{A cm}^{-2}$ in 1 M KCl.	46

4.12	Specific capacitance of TNTs 5 %, TNTs 25 % TNTs 50 %, TNTs 75 % and TNTs 100 % at various discharge current densities.	46
4.13	FESEM images of TNTs synthesised using various applied voltage: (a) 10 V, (b) 20 V, (c) 30 V and (d) 40 V in electrolyte containing $\text{NH}_4\text{F}/\text{EG}/5\% \text{H}_2\text{O}$ for 1 hr.	48
4.14	Tube diameter and wall thickness in function of applied voltage.	49
4.15	Cyclic voltammograms for TNTs synthesised using various applied voltage in electrolyte containing $\text{NH}_4\text{F}/\text{EG}/5\% \text{H}_2\text{O}$ for 1 hr at the scan rate of $5 \text{ mV s}^{-1}$ in 1 M KCl.	50
4.16	(a) Galvanostatic charge-discharge and (b) specific capacitance of TNTs synthesised using various applied voltage in electrolyte containing $\text{NH}_4\text{F}/\text{EG}/5\% \text{H}_2\text{O}$ for 1 hr at current density of $2 \mu\text{A cm}^{-2}$ in 1 M KCl.	51
4.17	FESEM images of TNTs synthesised using various anodisation time: (a) 30 min, (b) 60 min, (c) 90 min and (d) 120 min in electrolyte containing $\text{NH}_4\text{F}/\text{EG}/5\% \text{H}_2\text{O}$ at anodisation voltage of 40 V.	52
4.18	Cyclic voltammograms for TNTs synthesised at different anodisation time at the scan rate of $5 \text{ mV s}^{-1}$ in 1 M KCl.	53
4.19	(a) Galvanostatic charge-discharge and (b) specific capacitance of TNTs synthesised in in different anodisation time at current density of $2 \mu\text{A cm}^{-2}$ in 1 M KCl.	54
4.20	FESEM images of (a) TNTs, (b) R-TNTs and side views of (c) R-TNTs.	56
4.21	Colour transformation of (a) TNTs and (b) R-TNTs upon electrochemical reduction.	56
4.22	XRD patterns of (a) as-anodised TNTs (b) TNTs and (c) R-TNTs. Noted that A and Ti represent anatase and titanium, respectively.	57
4.23	Wide scan survey XPS spectrum of (a) TNTs and (b) R-TNTs.	58
4.24	(a) Ti 2p XPS spectra and (b) O 1s XPS spectra of TNTs and R-TNTs.	59
4.25	Cyclic voltammogram of TNTs and R-TNTs electrodes at the scan rate of $200 \text{ mV s}^{-1}$ .	60

4.26	Cyclic voltammogram of R-TNTs prepared at different (a) voltage and (b) duration conducted at the scan rate of $200 \text{ mV s}^{-1}$ , Specific capacitance of R-TNTs with respect to applied voltage (a') and duration (b').	62
4.27	Cyclic voltammogram of R-TNTs recorded at different scan rates 5 to $200 \text{ mV s}^{-1}$ .	62
4.28	Galvanostatic charge-discharge curves of the TNTs and R-TNTs conducted at the current density of $20 \mu\text{A cm}^{-2}$ .	63
4.29	Specific capacitance of R-TNTs at various discharge current densities.	64
4.30	Cyclic voltammogram of $\text{Na}_2\text{SO}_4$ and mixture of $\text{MnSO}_4$ and $\text{Na}_2\text{SO}_4$ at the scan rate of $20 \text{ mV s}^{-1}$ .	66
4.31	Cyclic voltammogram of $\text{Na}_2\text{SO}_4$ and mixture of $\text{CoSO}_4$ and $\text{Na}_2\text{SO}_4$ at the scan rate of $20 \text{ mV s}^{-1}$ .	67
4.32	A pulse scheme of on-time and off-time during pulse reverse electrodeposition.	68
4.33	FESEM images of $\text{Mn}_2\text{O}_3$ deposited onto R-TNTs at different applied potential: (a) $-0.60 \text{ V}$ , (b) $-0.70 \text{ V}$ , (c) $-0.80 \text{ V}$ and (d) $-0.90 \text{ V}$ using 10 % duty cycle for 5 min.	70
4.34	FESEM images of $\text{Co}_3\text{O}_4$ deposited onto R-TNTs using 10 % duty cycle for 5 min at different applied potential: (a) $-0.60 \text{ V}$ , (b) $-0.70 \text{ V}$ , (c) $-0.80 \text{ V}$ and (d) $-0.90 \text{ V}$ . Insert pictures are the high magnification of the samples.	71
4.35	Schematic representation of charge-transfer at low and high potential during electrodeposition	72
4.36	FESEM images of $\text{Mn}_2\text{O}_3$ deposited onto R-TNTs at different duty cycle: (a) 10 %, (b) 25 %, (c) 50 %, (d) 75 %, and (e) 90 % at $-0.90 \text{ V}$ for 5 min.	75
4.37	The output of the pulse deposition graph for a few selected cycles.	76
4.38	FESEM images of $\text{Co}_3\text{O}_4$ deposited onto R-TNTs at $-0.90 \text{ V}$ for 5 min using different duty cycle: (a) 10 %, (b) 25 %, (c) 50 %, (d) 75 %, and (e) 90 %.	77
4.39	FESEM images of $\text{Mn}_2\text{O}_3$ deposited into R-TNTs at different deposition time: (a) 5, (b) 10, (c) 15, (d) 20 and (e) 25 min at potential of $-0.90 \text{ V}$ using 10 % duty cycle.	79

4.40	Tube diameter and wall thickness in function of deposition time.	80
4.41	FESEM images of $\text{Co}_3\text{O}_4$ deposited onto R-TNTs at potential -0.90 V using 10 % duty cycle at different deposition time: (a) 5, (b) 10, (c) 15, (d) 20 and (e) 25 min.	81
4.42	FESEM images of $\text{Co}_3\text{O}_4$ deposited onto R-TNTs at -0.90 V using 10 % duty cycle for 5 min using different $\text{CoSO}_4$ electrolyte concentration: (a) 2 mM, (b) 5 mM, (c) 10 mM, (d) 15 mM and (e) 20 mM.	83
4.43	FESEM images of cross-sectional: (a) R-TNTs at low magnification (a') R-TNTs at high magnification, (b) $\text{Mn}_2\text{O}_3/\text{R-TNTs}$ at low magnification, (b') $\text{Mn}_2\text{O}_3/\text{R-TNTs}$ at high magnification, (c) $\text{Co}_3\text{O}_4/\text{R-TNTs}$ at low magnification and (c') $\text{Co}_3\text{O}_4/\text{R-TNTs}$ at high magnification	85
4.44	XRD patterns of (a) R- TNTs and (b) $\text{Mn}_2\text{O}_3/\text{R-TNTs}$ . Noted that the insert figures are the larger image of $\text{Mn}_2\text{O}_3$ peaks at 38.269 and 82.252 which overlap with Ti.	86
4.45	XRD patterns of (a) R-TNTs and (b) $\text{Co}_3\text{O}_4/\text{R-TNTs}$ .	87
4.46	TEM image of: (a) R-TNTs, (b) $\text{Mn}_2\text{O}_3/\text{R-TNTs}$ and (c) $\text{Co}_3\text{O}_4/\text{R-TNTs}$ .	88
4.47	Cyclic voltammograms for: (a) R-TNTs and $\text{Mn}_2\text{O}_3/\text{R-TNTs}$ and (b) R-TNTs and $\text{Co}_3\text{O}_4/\text{R-TNTs}$ deposited at different pulse potential using 10 % duty cycle for 5 min at the scan rate of 5 $\text{mV s}^{-1}$ in 1 M KCl. Insert image is a larger image of cyclic voltammograms for R-TNTs and $\text{Mn}_2\text{O}_3/\text{R-TNTs}$ deposited at -0.60, -0.70 and -0.80 V.	90
4.48	Cyclic voltammograms of (a) $\text{Mn}_2\text{O}_3/\text{R-TNTs}$ and (b) $\text{Co}_3\text{O}_4/\text{R-TNTs}$ deposited at pulse potential of -0.90 V at different scan rate in 1 M KCl.	92
4.49	Specific capacitance for $\text{Mn}_2\text{O}_3/\text{R-TNTs}$ and $\text{Co}_3\text{O}_4/\text{R-TNTs}$ deposited at pulse potential of -0.90 V with function of scan rate.	93
4.50	Galvanostatic charge-discharge of (a) R-TNTs and $\text{Mn}_2\text{O}_3/\text{R-TNTs}$ and (b) R-TNTs and $\text{Co}_3\text{O}_4/\text{R-TNTs}$ deposited at different pulse potential using 10 % duty cycle for 5 min at current density of 0.1 $\text{mA cm}^{-2}$ in 1 M KCl.	94
4.51	Galvanostatic charge-discharge of $\text{Mn}_2\text{O}_3/\text{R-TNTs}$ deposited at 10 % duty cycle at different current density in 1 M KCl.	96

4.52	Galvanostatic charge-discharge of $\text{Co}_3\text{O}_4/\text{R-TNTs}$ deposited at 10 % duty cycle at different current density in 1 M KCl. Insert picture is the larger image of charge-discharge curve of same sample at 0.3, 0.4 and 0.5 $\text{mA cm}^{-2}$ .	96
4.53	Specific capacitance of $\text{Mn}_2\text{O}_3/\text{R-TNTs}$ and $\text{Co}_3\text{O}_4/\text{R-TNTs}$ deposited at -0.90 V with function of current density.	97
4.54	Cyclic voltammograms of (a) R-TNTs and $\text{Mn}_2\text{O}_3/\text{R-TNTs}$ and (b) R-TNTs and $\text{Co}_3\text{O}_4/\text{R-TNTs}$ deposited using different duty cycle at -0.90 V for 5 min at the scan rate of 5 $\text{mV s}^{-1}$ in 1 M KCl.	99
4.55	Cyclic voltammograms of (a) $\text{Mn}_2\text{O}_3/\text{R-TNTs}$ and (b) $\text{Co}_3\text{O}_4/\text{R-TNT}$ deposited at 90 % duty cycle at scan rate of 5 $\text{mV s}^{-1}$ in 1 M KCl upon longer cycling process.	100
4.56	Galvanostatic charge-discharge of (a) R-TNTs and $\text{Mn}_2\text{O}_3/\text{R-TNTs}$ and (b) R-TNTs and $\text{Co}_3\text{O}_4/\text{R-TNTs}$ deposited using various duty cycle at -0.90 V for 5 min at current density of 0.1 $\text{mA cm}^{-2}$ in 1 M KCl.	101
4.57	Cyclic voltammograms of (a) R-TNTs and $\text{Mn}_2\text{O}_3/\text{R-TNTs}$ and (b) R-TNTs and $\text{Co}_3\text{O}_4/\text{R-TNTs}$ deposited at -0.90 V using 10 % duty cycle with various deposition time at the scan rate of 5 $\text{mV s}^{-1}$ in 1 M KCl.	103
4.58	Specific capacitance for $\text{Mn}_2\text{O}_3/\text{R-TNTs}$ deposited for 5 min and $\text{Co}_3\text{O}_4/\text{R-TNTs}$ deposited for 10 min with function of scan rate.	104
4.59	Galvanostatic charge-discharge of (a) R-TNTs and $\text{Mn}_2\text{O}_3/\text{R-TNTs}$ and (b) R-TNTs and $\text{Co}_3\text{O}_4/\text{R-TNTs}$ deposited at -0.90 V using 10 % duty cycle with various deposition time at current density of 0.1 $\text{mA cm}^{-2}$ in 1 M KCl.	105
4.60	Specific capacitance of $\text{Mn}_2\text{O}_3/\text{R-TNTs}$ deposited for 5 min and $\text{Co}_3\text{O}_4/\text{R-TNTs}$ deposited for 10 min in function of current density.	107
4.61	Cyclic voltammograms of (a) R-TNTs and $\text{Mn}_2\text{O}_3/\text{R-TNTs}$ and (b) R-TNTs and $\text{Co}_3\text{O}_4/\text{R-TNTs}$ deposited at -0.90 V using 10 % duty cycle for 5 min using different electrolyte concentration at the scan rate of 5 $\text{mV s}^{-1}$ in 1 M KCl.	108
4.62	Cyclic voltammograms of $\text{Co}_3\text{O}_4/\text{R-TNTs}$ deposited using 10 mM $\text{CoSO}_4$ at pulse potential of -0.90 V at different scan rate in 1 M KCl.	109

4.63	Galvanostatic charge-discharge of (a) R-TNTs and $\text{Mn}_2\text{O}_3/\text{R-TNTs}$ and (b) R-TNTs and $\text{Co}_3\text{O}_4/\text{R-TNTs}$ deposited at deposited at -0.90 V using 10 % duty cycle for 5 min using different electrolyte concentration at current density of $0.1 \text{ mA cm}^{-2}$ in 1 M KCl.	110
4.64	Cyclic voltammograms of (a) R-TNTs and $\text{Mn}_2\text{O}_3/\text{R-TNTs}$ and (b) R-TNTs and $\text{Co}_3\text{O}_4/\text{R-TNTs}$ deposited at deposited at -0.90 V using 10 % duty cycle for 5 min using different electrolyte pH at the scan rate of $5 \text{ mV s}^{-1}$ in 1 M KCl.	112
4.65	Galvanostatic charge-discharge of (a) R-TNTs and $\text{Mn}_2\text{O}_3/\text{R-TNTs}$ and (b) R-TNTs and $\text{Co}_3\text{O}_4/\text{R-TNTs}$ deposited at deposited at -0.90 V using 10 % duty cycle for 5 min using different electrolyte pH at current density of $0.1 \text{ mA cm}^{-2}$ in 1 M KCl.	114
4.66	Specific capacitance of (a) $\text{Mn}_2\text{O}_3/\text{R-TNTs}$ and (b) $\text{Co}_3\text{O}_4/\text{R-TNTs}$ deposited using various pH of metal precursor obtained from CV and galvanostatic charge-discharge at scan rate of $5 \text{ mV s}^{-1}$ current density of $0.1 \text{ mA cm}^{-2}$ .	115
4.67	Cyclic voltammograms of (a) R-TNTs and $\text{Mn}_2\text{O}_3/\text{R-TNTs}$ and (b) R-TNTs and $\text{Co}_3\text{O}_4/\text{R-TNTs}$ heated at various temperature at the scan rate of $5 \text{ mV s}^{-1}$ in 1 M KCl. Insert images cyclic voltammograms for $\text{Mn}_2\text{O}_3/\text{R-TNTs}$ and $\text{Co}_3\text{O}_4/\text{R-TNTs}$ deposited at 200, 300, 400 and 500 °C	117
4.68	Galvanostatic charge-discharge of (a) R-TNTs and $\text{Mn}_2\text{O}_3/\text{R-TNTs}$ and (b) R-TNTs and $\text{Co}_3\text{O}_4/\text{R-TNTs}$ heated at various temperature at current density of $0.1 \text{ mA cm}^{-2}$ in 1 M KCl.	118
4.69	Specific capacitance of (a) $\text{Mn}_2\text{O}_3/\text{R-TNTs}$ and (b) $\text{Co}_3\text{O}_4/\text{R-TNTs}$ heat at various temperature obtained from CV and galvanostatic charge-discharge at scan rate of $5 \text{ mV s}^{-1}$ current density of $0.1 \text{ mA cm}^{-2}$ .	119
4.70	Ragone plot of optimised TNTs, R-TNTs $\text{Mn}_2\text{O}_3/\text{R-TNTs}$ and $\text{Co}_3\text{O}_4/\text{R-TNTs}$ obtained at various current densities in 1.0 M KCl between -0.4 to 0.8 V. The insert image is larger plot of TNTs.	121
4.71	Variation of the specific capacitance of TNTs investigated in 1 M KCl at current density of $10 \text{ } \mu\text{A cm}^{-2}$ with respect to charge-discharge cycle number.	122
4.72	Variation of the specific capacitance of R-TNTs investigated in 1 M KCl at current density of $100 \text{ } \mu\text{A cm}^{-2}$ with respect to charge-discharge cycle number.	123

4.73	Variation of the specific capacitance of $\text{Mn}_2\text{O}_3/\text{R-TNTs}$ investigated in 1 M KCl at current density of $500 \mu\text{A cm}^{-2}$ with respect to charge-discharge cycle number.	123
4.74	Variation of the specific capacitance of $\text{Co}_3\text{O}_4/\text{R-TNTs}$ investigated in 1 M KCl at current density of $500 \mu\text{A cm}^{-2}$ with respect to charge-discharge cycle number.	124
4.75	Nyquist plot of TNTs in 1 M KCl as function of frequency	125
4.76	Nyquist plot of R-TNTs, $\text{Mn}_2\text{O}_3/\text{R-TNTs}$ and $\text{Co}_3\text{O}_4/\text{R-TNTs}$ in 1 M KCl as function of frequency.	125





## LIST OF ABBREVIATIONS AND SYMBOLS

ALD	Atomic Layer Deposition
CV	Cyclic voltammetry
DC	Direct Current
DI	Deionised Water
E	Energy Density
EDLC	Electric Double-Layer Capacitance
EDX	Energy Dispersive X-Ray Spectroscopy
EG	Ethylene Glycol
EIS	Electrochemical Impedance Spectroscopy
FESEM	Field Emission Scanning Electron Microscopy
IHP	Inner Helmholtz Plane
OHP	Outer Helmholtz Plane
P	Power Density
$R_{ct}$	Charge-transfer Resistance
$R_s$	Cell-electrolyte Resistance
R-TNTs	Reduced Titania Nanotubes
R-TNTs/ $Co_3O_4$	Reduced Titania Nanotubes/Cobalt Oxide
R-TNTs/ $Mn_2O_3$	Reduced Titania Nanotubes/ Manganese Oxide
SC	Specific Capacitance
$T_{on}$	On-time
$T_{off}$	Off-time
TEM	Transmission Electron Microscopy
TNTs	Titania Nanotubes



XPS X-Ray Photoelectron Spectroscopy

XRD X-Ray Diffraction Spectroscopy



## CHAPTER 1

### INTRODUCTION

#### 1.1 General Introduction

In response to the rapid development of the global economy, a fast growing market for portable electronic devices, the growing human population and the development of hybrid electric vehicles, the global energy consumption is accelerating at an alarming rate (Arico *et al.*, 2005; Chu *et al.*, 2012; Wang, *et al.*, 2012). The increasing of energy demand becomes unavoidable based on the current energy consumption rate. Therefore, the urge to develop energy storage system with high energy, high power, low-cost, and environmentally friendly have increased to satisfy the needs of modern society. Among various energy conversion and storage devices, supercapacitor, which is also known as electrochemical capacitor or ultracapacitor have attracted a great deal of attention from both industry and academia due to their unique characteristics that fill the gap between batteries and capacitors, by delivering higher power burst than batteries and storing more energy than capacitors. The device possesses remarkable characteristics as it is robust in withstanding hundred thousand of charging/discharging cycles without degrading. Supercapacitor has been undergoing rapid developments since the conception was proposed by Conway in the 1970s. The uprising of the researches on supercapacitor have given new hope in improvement of power of batteries (Simon *et al.*, 2008) which is desperately needed for many application such as cameras, cell phones, hybrid and electric vehicles.

Supercapacitor is characterised as electric double layer capacitors (EDLC) and pseudocapacitors. In EDLC, the capacitance of the material comes from the adsorption of both anions and cations at the electrode/electrolyte interface. Thus, it is strongly dependent on the surface area of the electrode materials that is accessible to the electrolyte ions (Huang *et al.*, 2015). In contrast to EDLC, pseudocapacitor stores energy through a faradaic process that involves fast and reversible redox reaction occurring at or near the electrode surface (Conway *et al.*, 2003).

The field of research and development of supercapacitor is currently focusing finding new materials which possess high capacitive performance and at the same time required minimal cost for the study. Countless effort have been done towards these criteria including mixing the oxides to become binary or ternary oxides, incorporating metal oxide with conducting polymer and compositing metal oxide with carbonaceous materials such as activated carbon, carbon nanotubes and graphene. Many attempts also have been done in adopting nanostructured materials for the use as supercapacitor. It is well noted that nanostructured material attributes high surface area which may contribute to higher capacitive performance due to the larger contact area between the

electrode/electrolyte. As reported in many literature, nanostructured materials indeed possess high electrical conductivity that makes them as a promising energy storage. Therefore, many efforts have been put to develop effective yet practical method synthesising the nanostructured oxide and hydroxide in various forms such as nanoparticles, nanotubes, nanorod, nanowire, nanosheets and others. Different methods have been applied by researchers such as precipitation (Chang *et al.*, 2015; Khalil, 2015), hydrothermal (Holi *et al.*, 2016; Myahkostupov *et al.*, 2011; Zaman *et al.*, 2012), sol-gel (Portet *et al.*, 2004), chemical bath deposition (Li *et al.*, 2011), anodisation (Macak *et al.*, 2006; Salari *et al.*, 2011a), electrospinning (Kim *et al.*, 2011), electrochemical deposition (Adelkhani *et al.*, 2010; Ali *et al.*, 2015; Kung *et al.*, 2012) and others.

Ever since Iijima discovered carbon nanotubes, (Iijima, 1991) one-dimensional (1D) nanostructured material has been widely explored. Although carbon is still the most explored nanotube material with fascinating properties, inorganic nanotubes (especially metal oxides or sulphides) are also widely studied to exploit their other material-specific properties and potential for biomedical, photochemical, electrical and environmental applications. Among all transition-metal oxides, titania is the most extensively studied material with more than 40 000 publications over the past 10 years, which makes titania as the most investigated compounds in materials science. Researchers have developed different preparative methods in synthesising 1D titania nanostructured including sol-gel method (Lakshmi *et al.*, 1997), template-assisted methods (Motonari *et al.*, 2000; Sander *et al.*, 2004), hydro/solvothermal method (Kasuga *et al.*, 1999), atomic layer deposition (ALD) (Shin *et al.*, 2004) and electrochemical anodisation method. Among various method introduced to synthesise titania nanotubes (TNTs), electrochemical anodisation method has been the most promising method as it offers suitably back-connected nanotubes on the Ti foil substrate which can be used directly as a binder-free supercapacitor electrode (Salari *et al.*, 2014).

However, it has been proclaimed that TNTs electrode suffered a very low specific capacitance (less than  $1 \text{ mF cm}^{-2}$ ) which resemble conventional electric double-layer capacitor (Salari *et al.*, 2011b) due to poor electrical conductivity (Wu *et al.*, 2014). Therefore, many attempts have been done to improve the capacitive performance of this material by thermal treatment (Lu *et al.*, 2012; Salari *et al.*, 2012), electrochemical doping approach (Wu *et al.*, 2014; Zhou *et al.*, 2013) and incorporation with metal oxides (Lu *et al.*, 2012; Xie *et al.*, 2009a; Xie *et al.*, 2009b) and conductive polymers (Mujawar *et al.*, 2011; Xie *et al.*, 2012; Xie *et al.*, 2014).

## 1.2 Problem Statement

The rapid growth of population and global economy has significantly increase the demand for energy consumption. Therefore, the urgency to find an energy storage that possess high energy, high power, low cost and environmentally friendly have become the 21<sup>st</sup> century problem. The current energy storage such as batteries can hold a large amount of power, however it have low cycle life and charge-discharge characteristics, while capacitor can charge almost instantly but suffered with low storage. As for our electric power future, we need to store and release large amount of electricity quickly

and quite likely supercapacitor possess both good values from batteries and capacitor. Supercapacitor is a high-capacity capacitor that attempts to combine the high power density of the conventional capacitors with the high energy density of a battery. This energy storage device also possess long cycle life and fast charge-discharge capability. Supercapacitor have attract significant attention mainly due to their numerous potential application as energy storage system in different field. The development of supercapacitor focuses on enhancing the capacitive performance of the material as well as power density, energy density and its life cycle.

Nanostructured material such as titania nanotubes have gain much attention as they possess high surface area which may contribute to higher capacitive performance (Lu *et al.*, 2012). Many researcher attempt to synthesis titania nanotubes in a powder form as they can easily modified by make it to binary or ternary metal oxide during the initial synthesis. Nevertheless, powder based sample is not practical to the industry. They needed to be further prepared as an electrode by adding binder and coated to a substrate. Therefore, in this study titania nanotubes were synthesised using anodisation method whereby the nanotubes were grown directly on the Ti substrate surface which make it as a binder less electrode and ready to be use. However, titania nanotubes was reported to have very low capacitive value which resemble conventional capacitor (Zhou *et al.*, 2016). To address this obstacle, many strategies have been done to improve the capacitive performance of titania nanotubes such as incorporation of metal oxides (Cui *et al.*, 2016; Kontos *et al.*, 2009; Xie *et al.*, 2008; Xie *et al.*, 2009b). However, some of the strategies requires intensive controlled condition, toxic chemical and long preparation time which leads to high cost for a large scale production. Therefore, it is crucial to find an alternative method that environmentally friendly, energy efficient and low cost. Modification through electrochemical technique is known to have these criteria and capable of producing surface of desired characteristics.

Countless efforts have been done using various electrodeposition method to deposit metal oxides onto the titania nanotubes. However, due to the overlapping of diffusion zones of the active ions during the electrodeposition leading to formation of larger metal oxide particle size which end up covering the nanotubes opening. In this work, pulse reverse electrodeposition method has been adopted to overcome this problem. In this method a series of pulse potential referred to as on-time separated by intervals of zero current potential (off-time) are applied which leads to formation of nano or quantum dot size particles evenly distributed as a compact crystalline structure. The effect of operating parameters of pulse reverse deposition of  $\text{Mn}_2\text{O}_3$  and  $\text{Co}_3\text{O}_4$  into titania nanotubes based on the capacitive performance have been performed. Up to this date there is no report on pulse reverse electrodeposition of  $\text{Mn}_2\text{O}_3$  and  $\text{Co}_3\text{O}_4$  into the modified titania nanotubes. Modification on titania nanotubes done in this work may provide new pathways in order to enhance the capacitive performance of titania nanotubes.

### 1.3 Background of Study

TNTs anodised from pure Ti foil are studied extensively as a potential supercapacitor electrode material due to its high surface area, high ion accessibility, controllable tube structure and relatively low cost. Moreover, vertically oriented TNTs standing directly on the current collector (Ti foil) have the advantages of eliminating contact impedance and reducing additional weight arising from the addition of conductive agent and binder. However, it was widely reported that TNTs possess a low specific capacitance  $\sim 50$  to  $911 \mu\text{F cm}^{-2}$  that impede their application on a large scale due to the poorer electrochemical activity and lower electronic conductivity (Huang *et al.*, 2016; Hui *et al.*, 2013). Although it is a transition metal oxide, TNTs are mostly considered as an EDLC capacitor due to its semiconducting nature, which limits the conductivity and prevents fast electron transfer. In this study, two major methods were adopted to enhance the electrochemical capacitance of the TNTs electrode. The first method was by electrochemical reduction of TNTs which demonstrates remarkable capacitance improvement of 40 to 60 times higher than the sole TNTs. The second method was by constructing hybrid arrays by utilising the unique tubular channels of the TNTs, which provide a regular architecture for feasible loading of various electroactive materials (for this study are  $\text{Mn}_2\text{O}_3$  and  $\text{Co}_3\text{O}_4$ ) (Wu *et al.*, 2014; Zhou *et al.*, 2014). This structure promotes the utilisation of these electroactive materials because of available large species and effective ion diffusion path for the electrochemical reactions. Prior to the modification, a study on influence of anodisation parameters to the morphology and architecture of the anodised TNTs was done to find the optimum condition for the synthesis of TNTs. Anodisation parameters such as electrolyte composition, anodisation voltage and time are varied throughout the study. The overview of the study was presented in Figure 1.1. Manganese oxide ( $\text{Mn}_2\text{O}_3$ ) and cobalt oxide ( $\text{Co}_3\text{O}_4$ ) are one of the pseudocapacitive materials with a large theoretical specific capacitance  $\sim 1300$  for  $\text{Mn}_2\text{O}_3$  and  $\sim 3560 \text{ F g}^{-1}$  for  $\text{Co}_3\text{O}_4$  (Huang *et al.*, 2015). Nevertheless, both metal oxides sustain the relatively low electrical conductivity which leads to the poor specific capacitance. One promising way is by incorporating the metal oxides into the electrically conductive skeleton to enhance its electrochemical performance. Therefore, in this study the TNTs was modified by electrochemical reduction method (sample denoted as R-TNTs) prior the incorporation with the metal oxides. Pulse reverse electrodeposition was used for the electrodeposition of  $\text{Mn}_2\text{O}_3$  and  $\text{Co}_3\text{O}_4$  onto the R-TNTs as it is considered a useful technique for the production of novel electroactive materials as it can tune in the electrodeposited material to the desired morphology.

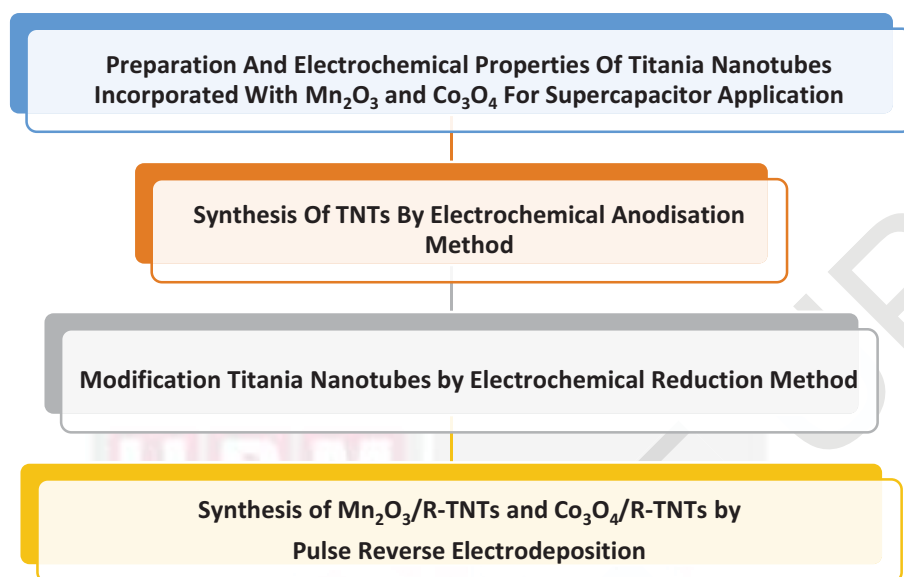


**Figure 1.1: Overview of the study.**

#### **1.4 Objectives of the Study**

The aim of this study is to prepare highly ordered titania nanotubes thin film and incorporate it with metal oxides in order to enhance the specific capacitance of the electrode. Several objectives were outlined towards the aim. Experimental works have been planned and done appropriately to ensure the smooth conduct towards the completion of the study. Therefore, the objectives of the study are as follow:

1. To synthesise highly ordered titania nanotubes thin film (TNTs) via electrochemical anodisation of titanium in mixture of ethylene glycol and water containing  $\text{NH}_4\text{F}$  solution.
2. To modify the TNTs thin films via electrochemical cathodic reduction.
3. To synthesise the manganese oxide doped modified titania nanotubes thin films ( $\text{Mn}_2\text{O}_3/\text{R-TNTs}$ ) and cobalt oxide doped modified titania nanotubes thin film ( $\text{Co}_3\text{O}_4/\text{R-TNTs}$ ) via pulse reverse electrodeposition method.
4. To evaluate the surface morphology and chemical states of TNTs, R-TNTs,  $\text{Mn}_2\text{O}_3/\text{R-TNTs}$  and  $\text{Co}_3\text{O}_4/\text{R-TNTs}$ .
5. To analyse the specific capacitance, power density and energy density of the prepared samples from galvanostatic charge-discharge tests.
6. To evaluate the electrochemical stability and coulombic efficiency of the samples through cycle stability tests.



## REFERENCES

- Adelkhani, H. and Ghaemi, M. 2010. Characterization of manganese dioxide electrodeposited by pulse and direct current for electrochemical capacitor. *Journal of Alloys and Compounds* 493: 175-178.
- Albu, S.P., Ghicov, A., Aldabergenova, S., Drechsel, P., LeClere, D., Thompson, G.E., Macak, J.M. and Schmuki, P. 2015. Formation of double-walled TiO<sub>2</sub> nanotubes and robust anatase membranes. *Advance Materials* 20:4135-4139.
- Ali, G.A.M., Yusoff, M.M., Ng, Y.H., Lim, H.N. and Chong, K.F. 2015. Potentiostatic and galvanostatic electrodeposition of manganese oxide for supercapacitor application: A comparison study. *Current Applied Physics* 15: 1143-1147.
- Alvi, F., Ram, M.K., Basnayaka, P.A., Stefannakos, E., Goswami, Y. and Kumar, A. 2011. Graphene-polyethylenedioxythiophene conducting polymer nanocomposite based supercapacitor. *Electrochimica Acta* 56: 9406-9412.
- Arico, A. S., Bruce, P., Scrosati, B., Tarascon, J. M. and Schalkwijk, W. V. 2015. Nanostructured materials for advanced energy conversion and storage devices. *Nature Materials*. 4: 366-377.
- Arbizzani, C., Beninati, S., Lazzari, M., Soavi, F. and Mastragostino, M. 2007. Electrode materials for ionic liquid-based supercapacitors. *Journal of Power Sources*. 174: 648-652.
- Arbizzani, C., Biso, M., Beninati, S., Lazzari, M., Soavi, F. and Mastragostino, M. 2008. Safe, high energy supercapacitors based on solvent-free ionic liquid electrolytes. *Journal of Power Sources*. 185: 1575-1579.
- Ataherian, F., Lee, K.T. and Wu, N.L. 2010. Long-term electrochemical behaviours of manganese oxide aqueous electrochemical capacitor under reducing potential. *Electrochimica Acta* 55: 7429-7435.
- Ayal, A.K., Zainal, Z., Lim, H.N., Talib, Z.A., Lim, Y.C., Chang, S.K., Samsudin, N.A., Holi, A.M. and Amin, W.N.M. 2016. Electrochemical deposition of CdSe-sensitized TiO<sub>2</sub> nanotubes arrays with enhance photoelectrochemical performance for solar cell application. *Journal of Material Science: Materials in Electronic* 27: 5204-5210.
- Bai, Y., Rakhi, R.B., Chen, W. and Alshareef, H.N. 2013. Effect of pH-induced chemical modification of hydrothermally reduced graphene oxide on supercapacitor performance. *Journal of Power Sources* 233: 313-319.
- Bard, A.J. and Faulkner, L.R. 2001. Electrochemical method: Fundamentals and applications 2<sup>nd</sup> edition. New York: John Wiley.

- Beranek, R., Hildebrand, H. and Schmuki, P. 2003. Self-organized porous titanium oxide prepared in  $\text{H}_2\text{SO}_4/\text{HF}$  electrolytes. *Electrochemical and Solid-State Letters* 6: B12-B14.
- Brownson, J.R.S. and Levy-Clement, C. 2009. Nanostructured  $\alpha$ - and  $\beta$ -cobalt hydroxide thin films. *Electrochimica Acta*. 54: 6637-6644.
- Chang, S.K., Zainal, Z., Tan, K.B., Yusof, N.A., Wan Yusoff, W.M.D. and Prabakaran, S.R.S. 2015. Synthesis of electrochemical properties of nanostructured nickel-cobalt oxides as supercapacitor electrodes in aqueous media. *International Journal of Energy Research* 39: 1366-1377.
- Chang, S.K., Zainal, Z., Tan, K.B., Yusof, N.A., Wan Yusoff, W.M.D. and Prabakaran, S.R.S. 2012. Nickel-cobalt oxide/activated carbon composite electrodes for electrochemical capacitors. *Current Applied Physics* 12: 1421-1428.
- Chang, J.K., Hsieh, W.C. and Tsai, W.T. 2008. Effect of Co content in the materials characteristics and supercapacitive performance of binary Mn-Co oxide electrodes. *Journal of Alloy and Compounds* 461: 667-674.
- Chee, W.K., Lim, H.N. and Huang, N.M. 2015. Electrochemical properties of free-standing polypyrrole/graphene oxide/zinc oxide flexible supercapacitor. *International Journal of Energy Research* 31: 111-119.
- Chen, X. Liu, L., Yu, P.Y. and Mao, S.S. 2011. Increasing solar absorption for photocatalysis with black hydrogenated titanium dioxide nanocrystals. *Science* 331: 746-750.
- Chu, S., and Majumdar, A. 2012 Opportunities and challenges for a sustainable energy future. *Nature*. 488: 294-303.
- Chung, C.M., Huang, C.W., Teng, H. and Ting, J.M. 2010. Effect of carbon nanotube grafting on the performance of electric double layer capacitors. *Energy & Fuels* 24: 6476-6482.
- Cochran, R.E., Shuye, J.J. and Padture, N.P. 2007. Template-based, near-ambient synthesis of crystalline metal-oxide nanotubes, nanowires and coaxial nanotubes. *Acta Materialia* 55: 3007-3014
- Conway, B.E. 1999. Electrochemical supercapacitor: Scientific fundamentals and technological applications. New York: Kulwer Academic/Plenum Publisher.
- Conway, B.E. and Pell, W.G. 2003. Double-layer and pseudocapacitance types of electrochemical capacitor and their applications to the development of hybrid devices. *Journal of Solid State Electrochemistry* 7: 637-644.



- Cui, L.H., Wang, Y., Shu, X., Zhang, J.F., Yu, C.P., Cui, J.W., Zheng, H.M., Zhang, Y. and Wu, C.Y. 2016. Supercapacitive performance of hydrogenated TiO<sub>2</sub> nanotube arrays decorated with nickel oxide nanoparticles. *RSC Advances* 6: 12185-12192.
- Dong, S., Chen, X., Gu, L., Zhou, X., Li, L., Liu, Z., Han, P., Xu, H., Yao, J., Wang, H., Zhang, X., Shang, C., Cui, G., and Chen, L. 2011. One dimensional MnO<sub>2</sub>/titanium nitride nanotube coaxial arrays for high performance electrochemical capacitive energy storage. *Energy and Environmental Science* 4: 3502-3508
- Du, G.H., Chen, Q., Che, R.C., Yuan, Z.Y. and Peng, L.M. 2001. Preparation and structure analysis of titanium oxide nanotubes. *Applied Physics Letters* 79: 3702-3704.
- Endut, Z., Hamdi, M. and Basirun, W.J. 2013. Optimization and functionalization of anodized titania nanotubes for redox supercapacitor. *Thin Solid Films* 549: 306-312.
- Frackowiak, E. and Béguin, F. 2001. Carbon materials for the electrochemical storage of energy in capacitors. *Carbon* 39: 937-950.
- Gamby, J., Taberna, P.L., Simon, P., Fauvarque, J.L. and Chesneau, M. 2001. Studies and characterization of various activated carbons used for carbon/carbon supercapacitor. *Journal of Power Sources* 101: 109-116.
- Gao, B., Li, X., Ma, Y., Cao, Y., Hu, Z., Zhang, Z., Fu, J., Huo, K., Chu, P.K. 2014. MnO<sub>2</sub>-TiO<sub>2</sub>/C nanocomposite arrays for high-performance supercapacitor electrode. *Thin Solid Films* 584: 61-65.
- Ghaemi, M. and Binder, L. 2002. Effects of direct and pulse current on electrodeposition of manganese dioxide. *Journal of Power Sources* 111: 248-254.
- Ghicov, A. and Schmuki, P. 2009. Self-ordering electrochemistry: A review on growth and functionality of TiO<sub>2</sub> nanotubes and other self-aligned MO<sub>x</sub> structures. *Chemical Communications* 20: 2791-2808.
- Gong, D., Grimes, C.A. Varghese, O.K., Hu, W., Singh, R.S., Chen, Z. and Dickey, E.C. 2001. Titanium oxide nanotube arrays prepared by anodic oxidation. *Journal of Materials Research* 16: 3331-3334.
- Gurav, K.V., Kim, Y.K., Shin, S.W., Suryawanshi, M.P., Tarwal, N.L., Ghorpade, U.V., Pawar, S.M., Vanalakar, S.A., Kim, I.Y., Yun, J.H., Patil, P.S. and Kim, J. H. 2015. Pulsed electrodeposition of Cu<sub>2</sub>ZnSnS<sub>4</sub> thin films: Effect of pulse potentials. *Applied Surface Science* 334: 192-196.
- Hamdy, M.S., Amrollahi, R. and Mul, G. 2012. Surface Ti<sup>3+</sup> containing (blue) titania: A unique photocatalysis with high activity and selectivity in visible light stimulate selective oxidation. *ACS Catalysis* 2: 2641-2647.

- Holi, A.M., Zainal, Z., Talib, Z.A., Lim, H.N., Yap, C.C., Chang, S.K. and Ayal, A.K. 2016. Effect of hydrothermal growth time on ZnO nanorod arrays photoelectrode performance. *Optik - International Journal for Light and Electron Optics* 127: 11111-11118.
- Hoyer, P. 1996. Formation of a titanium dioxide nanotube array. *Langmuir* 12: 1411-1413.
- Huang, M., Li, F., Dong, F., Zhang, Y.X. and Zhang, L.L. 2015. MnO<sub>2</sub>-based nanostructures for high-performance supercapacitors. *Journal of Materials Chemistry A* 3: 21380-21423.
- Huang, Y.G., Zhang, X.H., Chen, X.B., Wang, H.Q., Chen, J.R., Zhong, X.X. and Li, Q.Y. 2015. Electrochemical properties of MnO<sub>2</sub>-deposited TiO<sub>2</sub> nanotubes arrays 3D composite electrode for supercapacitors. *International Journal of Hydrogen Energy* 40: 14331-14337.
- Iijima, S. 1991. Helical microtubules of graphitic carbon. *Nature*, 354: 56-58.
- Inamdar, A.L., Kim, Y., Pawar, S.M., Kim, J.H., Im, H. and Kim, H. 2011. Chemically grown, porous, nickel oxide thin-film for electrochemical supercapacitors. *Journal of Power Sources* 196: 2393-2397.
- Jacob, G. M., and Zhitomirsky, I. 2008. Microstructure and properties of manganese dioxide films prepared by electrodeposition. *Applied Surface Science* 254: 6671-6676.
- Jagdale, A.D., Kumbhar, V.S., and Lokhande, C.D. 2013. Supercapacitive activities of potentiodynamically deposited nanoflakes of cobalt oxide (Co<sub>3</sub>O<sub>4</sub>) thin film electrode. *Journal of Colloid and Interface Science* 406:225-230
- Jang, K., Yu, S., Park, S.H., Kim, H.S. and Ahn, H. 2015. Intense pulsed light-assisted facile and agile fabrication of cobalt oxide/nickel cobaltite nanoflakes on nickel-foam for high performance supercapacitor applications. *Journal of Alloys and Compounds* 618: 227-232.
- Kandalkar, S.G., Lee, H.M., Chae, H. and Kim, C.K. 2011. Structural, morphological, and electrical characteristics of the electrodeposited cobalt oxide electrode for supercapacitor applications. *Materials Research Bulletin* 46: 48-51.
- Kasuga, T., Hiramatsu, M., Hoson, A., Sekino, T. and Niihara, K. 1998. Formation of titanium oxide nanotube. *Langmuir* 14: 3160-3163.
- Kasuga, T., Hiramatsu, M., Hoson, A., Sekino, T. and Niihara, K. 1999. Titania nanotubes prepared by chemical processing. *Advanced Materials* 11: 1307-1311.
- Khalil, M. I. 2015. Co-precipitation in aqueous solution synthesis of magnetite nanoparticles using iron(III) salts as precursors. *Arabian Journal of Chemistry* 8: 279-284.

- Kiamahalleh, M. V., Zein, S.H.S., Najafpour, G., Sata, S.A. and Buniran, S. 2012. Multiwalled carbon nanotubes based nanocomposites for supercapacitors: A review of electrode materials. *Nano*, 07: 1230002.
- Kim, I.D. and Rothschild, A. 2011. Nanostructured metal oxide gas sensors prepared by electrospinning. *Polymers for Advanced Technologies* 22: 318-325.
- Kim, J.H., Zhu, K., Yan, Y., Perkins, C.L. and Frank, A.L. 2010. Microstructure and pseudocapacitive properties of electrodes constructed of oriented NiO-TiO<sub>2</sub> nanotubes arrays. *Nano Letters* 10: 4099-4104.
- Kim, Y., Jung, J., Kim, S., & Chae, W. S. 2013. Cyclic Voltammetric and Chronoamperometric Deposition of CdS. *Materials Transactions* 54: 1467-1472.
- Knez, M., Nielsch, K. and Niinisto, L. 2007. Synthesis and surface engineering of complex nanostructures by atomic layer deposition. *Advanced Materials* 19: 3425-3438.
- Kontos, A.I., Likodimos, V., Stergiopoulos, T., Tsoukleris, D.S. and Falaras, P. 2009. Self-organized anodic TiO<sub>2</sub> nanotube arrays functionalized by iron oxide nanoparticles. *Chemistry of Materials* 21: 662-672.
- Kotz, R., and Carlen, M. 2000. Principles and applications of electrochemical capacitors. *Electrochimica Acta* 45: 2483-2498.
- Koza, J.A., He, Z., Miller, A.S. and Switzer, J.A. 2012. Electrodeposition of crystalline Co<sub>3</sub>O<sub>4</sub>-A catalyst for the oxygen evolution reaction. *Chemistry of Materials* 24: 3567-3573.
- Kung, C.W., Chen, H.W., Lin, C.Y., Vittal, R. and Ho, K.C. 2012. Synthesis of Co<sub>3</sub>O<sub>4</sub> nanosheets via electrodeposition followed by ozone treatment and their application to high-performance supercapacitors. *Journal of Power Sources*, 214: 91-99.
- Lakshmi, B.B., Dorhout, P.K. and Martin, C.R. 1997. Sol-gel template synthesis of semiconductor nanostructures. *Chemistry of Materials* 9: 857-862.
- Lee, J. and Jho, J.Y. 2011. Fabrication of highly ordered and vertically oriented TiO<sub>2</sub> nanotube arrays for ordered heterojunction polymer/inorganic hybrid solar cell. *Solar Energy Materials and Solar Cells* 95: 3152-3156.
- Lee, K.T. and Wu, N.L. 2008. Manganese oxide electrochemical capacitor with potassium poly(acrylate) hydrogel electrolyte. *Journal of Power Sources* 179: 430-434.
- Lee, K., Lee, J., Kim, H., Lee, Y., Kim, D., Schmuki, P. and Tak, Y. 2009. Effect of electrolyte conductivity on the formation of nanotubular TiO<sub>2</sub> photoanode for a dye-sensitized solar cell. *Journal of Korean Physical Society* 54: 1027-1031.

- Lee, S.H., Lee, H., Cho, M.S., Nam, J.D. and Lee, Y.K. 2013. Morphology and composition control of manganese oxide by the pulse reverse electrodeposition technique for high performance supercapacitors. *Journal of Materials Chemistry A* 1: 14606-14611.
- Leskela, M. and Ritala, M. 2003. Atomic layer deposition chemistry: Recent developments and future challenges. *Angewandte Chemie International Edition* 42: 5548-5554.
- Li, Y., Huang, K., Yao, Z., Liu, S. and Qing, X. 2011.  $\text{Co}_3\text{O}_4$  thin film prepared by a chemical bath deposition for electrochemical capacitors. *Electrochimica Acta* 56: 2140-2144.
- Lim, Y.C., Zulkarnain, Z., Mohd Zobir, H. and Tan, W.T. 2011. Fabrication of highly ordered tio nanotubes from fluoride containing aqueous electrolyte by anodic oxidation and their photoelectrochemical response. *Journal of Nanoscience and Nanotechnology* 11: 1-10.
- Lim, Y.C., Zulkarnain, Z., Mohd Zobir, H. and Tan, W.T. 2012. Effect of water content on structurel and photoelectrochemical properties of titania nanotubes synthesized in fluoride ethylene glycol electrolyte. *Advance Materials Research* 501:204-208.
- Liu, M., Chang, J., Sun, J. and Gao, L. 2013. Synthesis of porous NiO using  $\text{NaBH}_4$  dissolved in ethylene glycol as precipitant for high performance supercapacitor. *Electrochimica Acta* 107: 9-15.
- Liu, R. Duay, J., Lee, S.B. 2011. Heterogenous nanostructured electrode materials for electrochemical energy storage. *Chemical Communications* 47: 1384-1404.
- Liu, R.S., Zhang, L., Sun, X., Lui, H. and Zhang, J. 2012. Electrochemical technologies for energy storage and conversion.
- Long, J.W., Belanger, D., Brousse, T., Sugimoto, W., Sassin, M.B. and Crosnier, O. 2011. Asymmetric electrochemical capacitors-Stretching the limits of aqueous electrolytes. *MRS Bullitin* 36: 513-522.
- Long, J.W., Brousse, T., and B'elangerd, D. 2015. Electrochemical capacitors: Fundamentals to applications. *Journal f the Electrochemical Society* 5: Y3.
- Lu, X., Wang, G., Zahi, T., Yu, M., Gan, J., Tong, Y. and Li, Y. 2013. Hydrogenated  $\text{TiO}_2$  nanotubes arrays for supercapacitors. *Nano Letters* 12: 1690-1696.
- Lu, T., Pan, L., Li, H., Zhu, G., Lv, T., Liu, X., Sun, Z., Chen, T. and Chua, D.H.C. 2011. Microwave-assisted synthesis of graphene-ZnO nanocomposite for electrochemical capacitors. *Journal of Alloys and Compounds* 509: 5488-5492.
- Macak, J.M., Gong, B.G., Hueppe, M. and Schmuki, P. 2007. Filling the  $\text{TiO}_2$  nanotubes by self-doping and electrodeposition. *Advance Materials* 19: 3027-3031.

- Macak, J.M., and Schmuki, P. 2006. Anodic growth of self-organized anodic TiO<sub>2</sub> nanotubes in viscous electrolytes *Electrochimica Acta* 52: 1258-1264.
- Macak, J.M., Sirotna, K. and Schmuki, P. 2005. Self-organized porous titanium oxide prepared in Na<sub>2</sub>SO<sub>4</sub>/NaF electrolytes. *Electrochimica Acta* 50: 3679-3684.
- Macak, J. M., Tsuchiya, H., Ghicov, A., Yasuda, K., Hahn, R., Bauer, S. and Schmuki, P. (2007). TiO<sub>2</sub> nanotubes: Self-organized electrochemical formation, properties and applications. *Current Opinion in Solid State and Materials Science* 11: 3-18.
- Macak, J. M., Tsuchiya, Taveira, L., Aldabergerova, S. and Schmuki, P. 2005. Smooth anodic TiO<sub>2</sub> nanotubes. *Angewandte Chemie International Edition* 44: 7463-7465.
- Macak, J.M., Zlamal, M., Krysa, J. and Schmuki, P. 2007. Self-organized TiO<sub>2</sub> nanotube layers as highly efficient photocatalyst. *Small* 3: 300-304.
- Maggie, P., Oomman, K.V., Gopal, K.M., Craig, A.G. and Keat, G.O. 2006. Unprecedented ultra-high hydrogen gas sensitivity in undoped titania nanotubes. *Nanotechnology* 17: 398.
- Malik, A. and Ray, B.C. 2011. Evolution of principle and practice of electrodeposited thin film: A review on effect of temperature and sonication. *International Journal of Electrochemistry* 1-16.
- Mallouki, M., Tran-Van, F., Sarrazinn, C., Chevrot, C. and Fauvarque, J.F. 2009. Electrochemical storage of polypyrrole-Fe<sub>2</sub>O<sub>3</sub> nanocomposite in ionic liquids. *Electrochimica Acta* 54: 2992-2997.
- Marichy, C., Bechelany, M. and Pinna, N. 2012. Atomic layer deposition of nanostructured materials for energy and environmental applications. *Advanced Material* 24: 1017-1032.
- McCafferty, E. and Wightman, J.P. 1998. Determination of the concentration of surface hydroxyl group of metal oxide films by quantitative XPS method. *Surface and Interface Analysis* 26: 549-564.
- Mi, H., Zhang, X., Yang, S., Ye, X. and Luo, J. 2008. Polyaniline nanofibers as the electrode material for supercapacitors. *Materials Chemistry and Physics* 112: 127-131.
- Mi, H., Zhang, X., Ye, X. and Yang, S. 2008. Preparation and enhanced capacitance of core-shell polypyrrole/polyaniline composite electrode for supercapacitors. *Journal of Power Sources* 176: 403-409.
- Miller, J.M., Dunn, B., Tran, T.D. and Pekala, R.W. 1997. Deposition of ruthenium nanoparticles on carbon aerogels for high energy density supercapacitor electrodes. *Journal of Electrochemistry Society* 144: L309-L311.



- Mor, G.K., Varghese, O.K., Paulose, M., Shankar, K. and Grimes, C.A. 2006. A review on highly ordered, vertically oriented  $\text{TiO}_2$  nanotube arrays: Fabrication, material properties, and solar energy applications. *Solar Energy Materials and Solar Cells* 90: 2011-2075.
- Motonari, A., Yusuke, M., Makoto, H. and Susumu, Y. 2000. Formation of titania nanotubes with high photo-catalytic activity. *Chemistry Letters* 29: 942-943.
- Mujawar, S.H., Ambade, S.B., Battumur, T., Ambade, R.B. and Lee, S.H. 2011. Electropolymerization of polyaniline on titanium oxide nanotubes for supercapacitor application. *Electrochimica Acta* 56: 4462-4466.
- Myahkostupov, M., Zamkov, M. and Castellano, F.N. 2011. Dye-sensitized photovoltaic properties of hydrothermally prepared  $\text{TiO}_2$  nanotubes. *Energy and Environmental Science* 4: 998-1010.
- Nah Y.C., Shrestha, N.K., Kim, D., Albu S.P., Paramasivam, I. and Schmuki, P. 2010. Voltage induced self-peeling of initiation layers on self-organized  $\text{TiO}_2$ - $\text{WO}_3$  nanotubes and formation of oxide nanosheet rolls. *Electrochemical Solid-State Letter* 8: K73-K76.
- Ng, C.H., Lim, H.N., Lim, Y.S., Chee, W.K. and Huang, N.M. 2015. Fabrication of flexible polypyrrole/graphene oxide/manganese oxide supercapacitor. *International Journal of Energy Research* 39: 344-355.
- Nian, J.N. and Teng, H. 2006. Hydrothermal synthesis of single-crystalline anatase  $\text{TiO}_2$  nanorods with nanotubes as the precursor. *The Journal of Physical Chemistry B* 110: 4193-4198.
- Park, B.O., Lokhande, C.D., Park, H.S., Jung, K.D. and Joo, O.S. 2004. Performance of supercapacitor with electrodeposited ruthenium oxide film electrodes-effect of film thickness. *Journal of Power Sources* 134: 148-152.
- Pei, Z.X., Zhu, M.S., Huang, Y., Huang, Y., Xue, Q., Geng, H.Y. and Zhi, C. Y. 2016. Dramatically improved energy conversion and storage efficiencies by simultaneously enhancing charge transfer and creating active sites in  $\text{MnO}_x/\text{TiO}_2$  nanotube composite electrodes. *Nano Energy* 20: 254-263.
- Portet, C., Taberna, P.L., Simon, P. and Laberty-Robert, C. 2004. Modification of Al current collector surface by sol-gel deposit for carbon-carbon supercapacitor applications. *Electrochimica Acta* 49: 905-912.
- Pradhan, A.K. and Das, S. 2014. Pulse reverse electrodeposition of Cu-SiC nanocomposite coating: Effects of surfactants and deposition parameters. *Metallurgical and Materials Transactions A* 45A: 5708-5720.
- Ramadoss, A. and Kim, S.J. 2013. Improved activity of a graphene- $\text{TiO}_2$  hybrid electrode in an electrochemical supercapacitor. *Carbon* 63: 434-445.

- Regonini, D., Bowen, C.R., Jaroenworarluck, A. and Stevens, R. 2013. A review of growth mechanism, structure and crystallinity of anodized TiO<sub>2</sub> nanotubes. *Materials Science and Engineering: R: Reports* 74: 377-406.
- Regonini, D., Satka, A., Jaroenworarluck, A., Allsopp, D.W.E., Bowen, C.R. and Stevens, R. 2012. Factors influencing surface morphology of anodized TiO<sub>2</sub> nanotubes. *Electrochimica Acta* 74: 244-253.
- Roy, P., Berger, S. and Schmuki, P. 2011. TiO<sub>2</sub> Nanotubes: Synthesis and applications. *Angewandte Chemie International Edition* 50: 2904-2939.
- Ruiz, V., Santmaria, R., Granda, M. and Blanco, C. 2009. Long-term cycling of carbon-based supercapacitors in aqueous media. *Electrochimica Acta* 54: 4481-4486.
- Saha, B., Jana, S.K., Majumder, S., Satpati, B. and Banerjee, S. 2015. Selective growth of co-electrodeposited Mn<sub>2</sub>O<sub>3</sub>-Au spherical composite network towards enhanced non-enzymatic hydrogen peroxide sensing. *Electrochimica Acta* 174: 853-863.
- Salari, M., Aboutalebi, S.H., Konstantinov, K. and Liu, H.K. 2011. A highly ordered titania nanotube array as a supercapacitor electrode. *Physical Chemistry Chemical Physics* 13: 5038-5041.
- Salari, M., Aboutalebi, S.H., Chidembo, A.T., Nevirkovets, I.P., Konstantinov, K. and Liu, H.K. 2012. Enhancement of electrochemical capacitance of TiO<sub>2</sub> nanotubes arrays through controlled phase transformation of anatase to rutile. *Physical Chemistry Chemical Physics* 14: 4770-4779.
- Salari, M., Aboutalebi, S.H., Chidembo, A.T., Konstantinov, K. and Liu, H.K. 2014. Surface engineering of self ordered TiO<sub>2</sub> nanotube arrays: A practical route towards energy storage applications. *Journals of Alloys and Compounds* 586: 197-201.
- Salari, M., Aboutalebi, S.H., Konstantinov, K. and Liu, H.K. 2011. Enhancement of the capacitance of TiO<sub>2</sub> nanotubes through controlled introduction of oxygen vacancies. *Journal of Materials Chemistry* 21: 5128-5133.
- Sander, M.S., Cote, M.J., Gu, W., Kile, B.M. and Tripp, C.P. 2004. Template-assisted fabrication of dense, aligned arrays of titania nanotubes with well-controlled dimensions on substrates. *Advanced Materials* 16: 2052-2057.
- Shin, H., Jeong, D.K., Lee, J., Sung, M.M. and Kim, J. 2004. Formation of TiO<sub>2</sub> and ZrO<sub>2</sub> nanotubes using atomic layer deposition with ultraprecise control of the wall thickness. *Advanced Materials* 16: 1197-1200.
- Simon, P. and Gogotsi, Y. 2008. Materials for electrochemical capacitors. *Nature Materials* 7: 845-854.

- Sulka, D.G., Kapusta-Kolodziej, J., Brzozka, A. and Jaskula, M. 2013. Anodic growth of TiO<sub>2</sub> nanopore arrays at various temperatures. *Electrochimica Acta* 104: 526-535.
- Shukla, A.K., Sampath, S., Vijayamohanan, K. 2000. Electrochemical supercapacitor: Energy storage beyond batteries. *Current Science* 79: 1656-1661.
- Sreekantan, S., Saharudin, K.A., Lockman, Z. and Tzu, T.W. 2010. Fast-rate formation of TiO<sub>2</sub> nanotubes arrays in an organic bath and their application in Photocatalysis. *Nanotechnology* 21: 365603.
- Tsai, C.C., Nian, J.N. and Teng, H. 2006. Mesoporous nanotube aggregates obtained from hydrothermally treating TiO<sub>2</sub> with NaOH. *Applied Surface Science* 253: 1898-1902.
- Tsuchiya, H. Macak, J.M., Taveira, L., Balaur, E., Ghicov, A., Sirotna, K. and Schmuki, P. (2005) Self-organized TiO<sub>2</sub> nanotubes prepared in ammonium fluoride containing acetic acid electrolytes. *Electrochemistry Communications* 7: 576-580.
- Wang, D., Liu, Y., Yu, B., Zhou, F. and Liu, W. 2009. TiO<sub>2</sub> nanotubes with tunable morphology, diameter and length: Synthesis and photo-electrical/catalytic performance. *Chemistry and Materials* 21: 1198-1206.
- Wang, G., Zhang, L. and Zhang, J. 2012. A review of electrode materials for electrochemical supercapacitors. *Chemical Society Reviews* 41: 797-828.
- Wang, J. 2006. Analytical Electrochemistry, Second Edition. New York: Wiley-VCH Publisher.
- Wei, W., Cui, X., Chen, W. and Ivey, D.G. 2011. Manganese oxide-based materials as electrochemical supercapacitor electrodes. *Chemical Society Reviews* 40: 1697-1721.
- Wei, D. and Ng, T.W. 2009. Application of novel room temperature ionic liquids in flexible supercapacitors. *Electrochemistry Communications* 11:1996-1999.
- Wu, H., Li, D., Zhu, X., Yang, C., Liu, D., Chen, X., Song, Y. and Lu, L. (2014). High-performance and renewable supercapacitors based on TiO<sub>2</sub> nanotube array electrodes treated by an electrochemical doping approach. *Electrochimica Acta* 116: 129-136.
- Wu, M.S. 2005. Electrochemical capacitance from manganese oxide nanowire structure synthesized by cyclic voltammetry electrodeposition. *Applied Physics Letters* 87: 153102.
- Xie, Y. and Du, H. 2012. Electrochemical capacitance performance of polypyrrole-titanium nanotube hybrid. *Journal of Solid State Electrochemistry* 16: 2683-2689.



- Xie, Y. and Fang, X. 2014. Electrochemical flexible supercapacitor based on manganese dioxide-titanium nitride nanotube hybrid. *Electrochimica Acta* 120: 273-283.
- Xie, Y. and Fu, D. 2010. Supercapacitance of ruthenium oxide deposited on titania and titanium substrates. *Materials Chemistry and Physics* 122: 23-29.
- Xie, Y., Huang, C., Zhou, L., Liu, Y. and Huang, H. 2009. Supercapacitor application of nickel oxide-titania nanocomposites. *Composites Science and Technology* 69: 2108-2114.
- Xie, Y., Zhou, L., Huang, C., Huang, H. and Lu, J. 2008. Fabrication of nickel oxide-embedded titania nanotube array for redox capacitance application. *Electrochimica Acta* 53: 3643-3649.
- Xie, Y., Zhou, L., Huang, C., Liu, Y. and Lu, J. 2009. Preparation and electrochemical capacitance of ruthenium oxide-titania nanotube composite. *Materials Science Forum* 614: 235-241.
- Xu, B., Hou, S., Cao, G., Wu, F. and Yang, Y. 2012. Sustainable nitrogen-doped porous carbon with high surface areas prepared from gelatin for supercapacitors. *Journal of Materials Chemistry* 22: 19088-19093.
- Xu, H., Zhang, Q., Zheng, C., Yan, W. and Chu, W. 2011. Application of ultrasonic wave to clean the surface of the TiO<sub>2</sub> nanotubes prepared by the electrochemical anodization. *Applied Surface Science* 257: 8478-8480.
- Yang, D. 2011. Pulsed laser deposition of manganese oxide thin films for supercapacitor applications. *Journal of Power Sources* 196: 8843-8849.
- Yang, P. and Mai, W. 2014. Flexible solid-state electrochemical supercapacitors. *Nano Energy* 8: 274-290.
- Yang, Z., Xu, F., Zhang, W., Mei, Z., Pei, B. and Zhu, X. 2014. Controllable preparation of multishelled NiO hollow nanosphere via layer-by-layer self-assembly for supercapacitor application. *Journal of Power Sources* 246: 24-31.
- Yohannes, W., Belenow, S.V., Guterman, V.E., Skibina, L.M., Volotchaec, V.A. and Lyanguzov, N.V. 2015. Effect of ethylene glycol on electrochemical and morphological features of platinum electrodeposits from chloroplatinic acid. *Journal of Applied Electrochemistry* 45: 623-633.
- Yu, Z., Tetard, L., Zhai, L. and Thomas, J. 2015. Supercapacitor electrode materials: nanostructures from 0 to 3 dimensions. *Energy & Environmental Science* 8: 702-730.
- Zaman, A.C., Ustundag, C.B., Kaya, F. and Kaya, C. 2012. Synthesis and electrophoretic deposition of hydrothermally synthesized multilayer TiO<sub>2</sub> nanotubes on conductive filters. *Materials Letters* 66: 179-181.

- Zhang, S., Peng, L.M., Chen, Q., Du, G.H., Dawson, G. and Zhou, W.Z. 2003. Formation mechanism of  $\text{H}_2\text{Ti}_3\text{O}_7$  nanotubes. *Physical Review Letters*, 91: 256103.
- Zhong, W.J., Sang, S.B., Liu, Y.Y., Wu, Q.M., Liu, K.Y. and Liu, H.T. 2015. Electrochemically conductive treatment of  $\text{TiO}_2$  nanotubes arrays in  $\text{AlCl}_3$  aqueous solution for supercapacitors. *Journal of Power Sources* 294: 216-222.
- Zhou, H. and Zhang, Y. 2014. Enhanced electrochemical performance of manganese dioxide spheres deposited on a titanium dioxide nanotube arrays substrate. *Journal of Power Sources* 272: 866-879.
- Zhou, H. and Zhang, Y. 2013. Enhanced the capacitance of  $\text{TiO}_2$  nanotubes arrays by a facile cathodic reduction process. *Journal of Power Sources* 239: 128-131.
- Zhou, H., Zou, X. and Zhang, Y. 2016. Fabrication of  $\text{TiO}_2@\text{MnO}_2$  nanotube arrays by pulsed electrodeposition and their application for high-performance supercapacitors. *Electrochimica Acta* 192: 259-267.
- Zwilling, V., Aucouturier, M. and Darque-Ceretti, E. 1999. Anodic oxidation of titanium and  $\text{TA}_6\text{V}$  alloy in chromic media. An electrochemical approach. *Electrochimica Acta* 45: 921-929.